Engineering Analysis with Boundary Elements ▮ (▮▮▮▮) ▮▮▮–▮▮▮

Contents lists available at ScienceDirect

Engineering Analysis with Boundary Elements

journal homepage: www.elsevier.com/locate/enganabound

On the spurious eigensolutions for the real-part boundary element method

J.T. Chen [a,b,*], J.W. Lee [a,b], Y.C. Cheng [a,b]

[a] Department of Harbor and River Engineering, National Taiwan Ocean University, Keelung 20224, Taiwan

[b] Department of Mechanical and Mechatronic Engineering, National Taiwan Ocean University, Keelung 20224, Taiwan

ARTICLE INFO

Article history:
Received 28 October 2007
Accepted 6 July 2008

Keywords:
Spurious eigenvalues
SVD
CHEEF
MRM

ABSTRACT

In this paper, the eigensolutions are derived by using seven determinants of the direct-searching approach. Seven determinants include the complex valued, real and imaginary parts of determinant using the complex-valued kernel as well as the determinant by using the real-part, and imaginary-part kernels and the multiple reciprocity method (MRM). It is found that spurious eigensolutions of the real-part BEM match well with those of the MRM for the one-dimensional case. To satisfy the time-domain causal constraint, it is found that the real-part and imaginary-part kernels are not fully independent but are governed by the Hilbert transform. The idea of the combined Helmholtz exterior integral equation formulation method (CHEEF) in conjunction with the singular value decomposition (SVD) technique can be applied to suppress the occurrence of spurious eigenvalues. Updating terms and updating documents are employed to extract out the true and spurious eigenvalues. Possible failure CHEEF points are also examined. Also, the SVD structure of four influence matrices are examined. It is found that true and spurious eigenvectors are imbedded in the right and left unitary vectors in the SVD. Two- and three-dimensional cases are straightforward to be extended. The Hilbert transform pair for real and imaginary kernels was also examined.

1. Introduction

The application of eigenanalysis is gradually increasing for vibration and acoustics. The demand for eigenanalysis calls for an efficient and reliable method of computation for eigenvalues and eigenmodes. Over the last three decades since 1974, several boundary element formulations have been employed to solve the eigenproblems [1], e.g., determinant searching method, internal cell method, dual reciprocity method, particular integral method and multiple reciprocity method. In this paper, we will focus on the direct determinant searching method with emphasis on spurious eigenvalues due to the real-part BEM and the multiple reciprocity method (MRM).

Spurious and fictitious frequencies stem from non-uniqueness solution problems. They appear in different aspects in computational mechanics. First of all, hourglass modes in the finite element method (FEM) using the reduced integration occur due to the rank deficiency [2]. Also, loss of divergence-free constraint for the incompressible elasticity also results in spurious modes. In the other side of numerical solution for the differential equation using the finite difference method (FDM), the spurious eigenvalue also appears due to discretization [3–5]. In the real-part BEM [6] or the MRM formulation [7–12], spurious eigensolutions occur in solving eigenproblems. Even though the complex-valued kernel is adopted, the spurious eigensolution also occurs for the multiply connected problem [13] as well as the appearance of fictitious frequency for the exterior acoustics [14]. Spurious solutions and fictitious frequencies in the integral formulation belong to spectral pollution since it cannot be suppressed by mesh refinement. The origin of spurious modes arises from an improper approximation of null space of the integral operator [15]. In this paper, a simple case of one-dimensional (1-D) rod will be demonstrated to see how spurious eigensolutions occur and how they can be suppressed. Although the 1-D case is simple [16–20], it provides the insight to understand how the spurious eigenvalue behaves and how they can be suppressed from the education point of view.

In the literature review, we can find seven alternatives to solve eigenproblems by using the direct-searching scheme. Tai and Shaw [21] employed the determinant of complex-valued BEM. De Mey [22] revisited this problem in 1976. Later, De Mey [23] proposed a simplified approach by using only the real-part or imaginary-part kernel where he found that spurious solutions were imbedded as well as the ill-posed matrix appeared. In a similar way of using the real-part kernel, Hutchinson [24,25] solved the free vibration of plate. Also, Yasko [26] as well as Duran et al. [27] employed the real-part kernel approach. It is interesting

* Corresponding author at: Department of Harbor and River Engineering, National Taiwan Ocean University, Keelung 20224, Taiwan.
E-mail address: jtchen@mail.ntou.edu.tw (J.T. Chen).

0955-7997/$ - see front matter © 2008 Published by Elsevier Ltd.
doi:10.1016/j.enganabound.2008.07.003

Table 1
Literature review for eigenproblems using the direct searching scheme in BEM

	1974	1976	1977	1985	1997	1999	2000	2001	Present
Indicator 1 det[C]	Tai and Shaw	De Mey						Duran et al.	✓
Indicator 2 Abs{det[C]}		De Mey							✓
Indicator 3 Im{det[C]}	Tai and Shaw								✓
Indicator 4 Re{det[C]}	Tai and Shaw								✓
Indicator 5 det[I]	Tai and Shaw		De Mey			Kang et al.			✓
Indicator 6 det[R]	Tai and Shaw		De Mey	Hutchinson and Wong			Yasko	Duran et al.	✓
Indicator 7 MRM					Chen and Wong	Yeih et al.			✓

to find that Kang et al. [28] proposed an imaginary-part kernel approach using the collocation approach as commented by Chen et al. [29]. Yeih et al. [9] found that the MRM is nothing but the real-part BEM. This is the reason why spurious eigenvalues are inherent in the two methods. The chronology list of the literature survey is shown in Table 1. All the indicators in the determinant searching method will be employed to solve a simple 1-D problem in this paper.

In the recent years, the singular value decomposition (SVD) technique has been applied to solve problems of continuum mechanics [30] and fictitious-frequency problems [14]. Two ideas, updating term and updating document [14], were successfully applied to extract the true and spurious solutions, respectively. Also, the CHIEF [31] and combined Helmholtz exterior integral equation formulation method (CHEEF) [32] methods were employed to suppress the occurrence of fictitious frequency and spurious eigenvalue, respectively. Based on these successful experiences, the SVD updating technique in conjunction with the CHEEF concept will be employed to study the spurious eigenvalue of the 1-D eigenproblem.

In this paper, eigenproblems of 1-D case will be explored by using seven indicators for the direct-searching scheme in details. Spurious modes in the real-part BEM formulation will be derived through the SVD technique and will be suppressed by using the CHEEF idea. The SVD structure for the four influence matrices in the dual BEM will be examined. Although a 1-D case is studied analytically, two- and three-dimensional (2-D and 3-D) cases will be straightforward extended by only changing the degenerate kernel.

The rest of this paper is organized as follows. In Section 2, we propose a dual formulation for the eigenproblem of a rod. In Section 3, seven indicators for the direct-searching scheme are employed to solve eigenproblems. The occurrence of spurious eigenvalues are suppressed by using the SVD technique in conjunction with the CHEEF idea in Section 4. Section 5 shows the updating terms and updating document to extract out true and spurious eigenvalues. Besides, SVD structure of the influence matrices are examined. Section 6 extends the 1-D case to 2-D and 3-D cases. Finally, a conclusion is made.

2. Dual formulation for one-dimensional eigenproblems

Consider the eigenproblems of free vibration for a rod subject to boundary conditions as shown in Figs. 1(a)–(c) with the following governing equation:

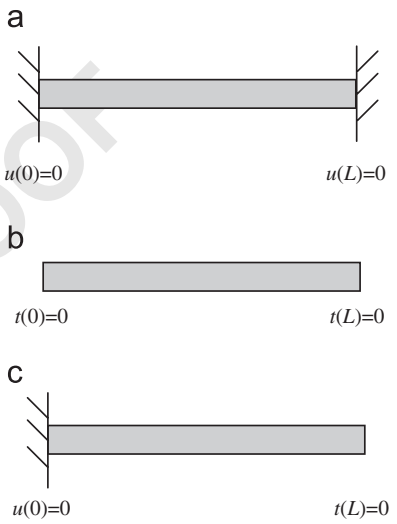

Fig. 1. (a) A rod subject to the Dirichlet BC (fixed end), (b) a rod subject to the Neumann BC (free end) and (c) a rod subject to the mixed-type BC.

$$\frac{d^2u(x)}{dx^2} + k^2u(x) = 0, \quad x \in D, \tag{1}$$

where $u(x)$ is the axial displacement of the rod, k is the wave number, D is the domain of $0<x<L$.

Three cases of boundary conditions are considered in Figs. 1(a)–(c) as follows:

Case 1: $u(0) = 0$ and $u(L) = 0$ (Dirichlet BC),
Case 2: $t(0) = 0$ and $t(L) = 0$ (Neumann BC),
Case 3: $u(0) = 0$ and $t(L) = 0$ (mixed-type BC),where $t(x_0) = du(x)/dx|_{x=x_0}$. By introducing the auxiliary system of the fundamental solution, we have

$$\frac{\partial^2U(x,s)}{\partial x^2} + k^2U(x,s) = \delta(x-s), \quad -\infty<x<\infty, \tag{2}$$

where δ is the Dirac-delta function, x is the field point, and s is the source point, $U(x,s)$ is a complex-valued fundamental solution as shown below:

$$U(x,s) = \frac{-1}{2ik}e^{-ik|x-s|} \tag{3}$$

Please cite this article as: Chen JT, et al. On the spurious eigensolutions for the real-part boundary element method. Eng Anal Bound Elem (2008), doi:10.1016/j.enganabound.2008.07.003

and can be expressed in terms of degenerate kernel

$$U(x,s)=\begin{cases}\dfrac{-1}{2ik}e^{ikx}e^{-iks}, & x<s,\\ \dfrac{-1}{2ik}e^{-ikx}e^{iks}, & x>s.\end{cases} \tag{4}$$

By employing the Green's third identity and integrating by parts, we derive the dual boundary integral equations as [33–36]

$$u(s)=\left[\frac{\partial U(x,s)}{\partial x}u(x)-U(x,s)t(x)\right]\Big|_{x=0}^{x=L}, \quad 0<s<L. \tag{5}$$

Then we exchange x with s to each other of Eq. (5), and obtain

$$u(x)=\left[\frac{\partial U(s,x)}{\partial s}u(s)-U(s,x)t(s)\right]\Big|_{s=0}^{s=L}, \quad 0<x<L. \tag{6}$$

By differentiating Eq. (6) with respect to the field point x, the dual boundary integral equations are shown below:

$$u(x)=[T(s,x)u(s)-U(s,x)t(s)]|_{s=0}^{s=L}, \quad 0<x<L, \tag{7}$$

$$t(x)=[M(s,x)u(s)-L(s,x)t(s)]|_{s=0}^{s=L}, \quad 0<x<L, \tag{8}$$

where the four kernels are shown in Table 2 and are defined as

$$T(s,x)=\frac{\partial U(s,x)}{\partial s}, \tag{9}$$

$$L(s,x)=\frac{\partial U(s,x)}{\partial x}, \tag{10}$$

$$M(s,x)=\frac{\partial U(s,x)}{\partial x\partial s}, \tag{11}$$

Conventionally, collocation of the field point x close to the boundary 0^+ and L^- for Eqs. (7) and (8) yields

$$[1+T(0,0^+)]u(0)-T(L,0^+)u(L) - U(0,0^+)t(0)+U(L,0^+)t(L)=0, \tag{12}$$

$$T(0,L^-)u(0)+[1-T(L,L^-)]u(L) - U(0,L^-)t(0)+U(L,L^-)t(L)=0, \tag{13}$$

$$M(0,0^+)u(0)-M(L,0^+)u(L) + [1-L(0,0^+)]t(0)+L(L,0^+)t(L)=0, \tag{14}$$

$$M(0,L^-)u(0)-M(L,L^-)u(L) - L(0,L^-)t(0)+[1+L(L,L^-)]t(L)=0. \tag{15}$$

By assembling the former two Eqs. (12) and (13) and the latter two Eqs. (14) and (15) into a matrix form, we have

$$\begin{bmatrix}1+T(0,0^+) & -T(L,0^+)\\ T(0,L^-) & 1-T(L,L^-)\end{bmatrix}\begin{Bmatrix}u(0)\\ u(L)\end{Bmatrix} + \begin{bmatrix}-U(0,0^+) & U(L,0^+)\\ -U(0,L^-) & U(L,L^-)\end{bmatrix}\begin{Bmatrix}t(0)\\ t(L)\end{Bmatrix}=\begin{Bmatrix}0\\ 0\end{Bmatrix}, \tag{16}$$

Table 2
Degenerate kernels for the free vibration of rod

Domain	Kernels			
	$U(s,x)$	$T(s,x)$	$L(s,x)$	$M(s,x)$
$x<s$	$\frac{-1}{2ik}e^{ik(x-s)}$	$\frac{1}{2}e^{ik(x-s)}$	$-\frac{1}{2}e^{ik(x-s)}$	$\frac{ik}{2}e^{ik(x-s)}$
$x>s$	$\frac{-1}{2ik}e^{-ik(x-s)}$	$-\frac{1}{2}e^{-ik(x-s)}$	$\frac{1}{2}e^{-ik(x-s)}$	$\frac{ik}{2}e^{-ik(x-s)}$

$$\begin{bmatrix}M(0,0^+) & -M(L,0^+)\\ M(0,L^-) & -M(L,L^-)\end{bmatrix}\begin{Bmatrix}u(0)\\ u(L)\end{Bmatrix} + \begin{bmatrix}1-L(0,0^+) & L(L,0^+)\\ -L(0,L^-) & 1+L(L,L^-)\end{bmatrix}\begin{Bmatrix}t(0)\\ t(L)\end{Bmatrix}=\begin{Bmatrix}0\\ 0\end{Bmatrix}. \tag{17}$$

Substituting the appropriate kernel functions shown in Table 2 into Eqs. (16) and (17), we have

$$\begin{bmatrix}\frac{1}{2} & -\frac{1}{2}e^{-ikL}\\ -\frac{1}{2}e^{-ikL} & \frac{1}{2}\end{bmatrix}\begin{Bmatrix}u(0)\\ u(L)\end{Bmatrix} + \begin{bmatrix}\frac{1}{2ik} & -\frac{1}{2ik}e^{-ikL}\\ \frac{1}{2ik}e^{-ikL} & -\frac{1}{2ik}\end{bmatrix}\begin{Bmatrix}t(0)\\ t(L)\end{Bmatrix}=\begin{Bmatrix}0\\ 0\end{Bmatrix}, \tag{18}$$

$$\begin{bmatrix}\frac{ik}{2} & -\frac{ik}{2}e^{-ikL}\\ \frac{ik}{2}e^{-ikL} & -\frac{ik}{2}\end{bmatrix}\begin{Bmatrix}u(0)\\ u(L)\end{Bmatrix} + \begin{bmatrix}\frac{1}{2} & -\frac{1}{2}e^{-ikL}\\ -\frac{1}{2}e^{-ikL} & \frac{1}{2}\end{bmatrix}\begin{Bmatrix}t(0)\\ t(L)\end{Bmatrix}=\begin{Bmatrix}0\\ 0\end{Bmatrix}. \tag{19}$$

After substituting boundary conditions of the three cases into Eqs. (18) and (19), we have the dual matrices of *UT* and *LM* equations.

For the case 1 with $u(0)=0$ and $u(L)=0$, we have

UT equation:

$$\begin{bmatrix}\frac{1}{2ik} & -\frac{1}{2ik}e^{-ikL}\\ \frac{1}{2ik}e^{-ikL} & -\frac{1}{2ik}\end{bmatrix}\begin{Bmatrix}t(0)\\ t(L)\end{Bmatrix}=\begin{Bmatrix}0\\ 0\end{Bmatrix}, \tag{20}$$

LM equation:

$$\begin{bmatrix}\frac{1}{2} & -\frac{1}{2}e^{-ikL}\\ -\frac{1}{2}e^{-ikL} & \frac{1}{2}\end{bmatrix}\begin{Bmatrix}t(0)\\ t(L)\end{Bmatrix}=\begin{Bmatrix}0\\ 0\end{Bmatrix}. \tag{21}$$

For the case 2 with $t(0)=0$ and $t(L)=0$, we have

UT equation:

$$\begin{bmatrix}\frac{1}{2} & -\frac{1}{2}e^{-ikL}\\ -\frac{1}{2}e^{-ikL} & \frac{1}{2}\end{bmatrix}\begin{Bmatrix}u(0)\\ u(L)\end{Bmatrix}=\begin{Bmatrix}0\\ 0\end{Bmatrix}, \tag{22}$$

LM equation:

$$\begin{bmatrix}\frac{ik}{2} & -\frac{ik}{2}e^{-ikL}\\ \frac{ik}{2}e^{-ikL} & -\frac{ik}{2}\end{bmatrix}\begin{Bmatrix}u(0)\\ u(L)\end{Bmatrix}=\begin{Bmatrix}0\\ 0\end{Bmatrix}. \tag{23}$$

For the case 3 with $u(0)=0$ and $t(L)=0$, we have

UT equation:

$$\begin{bmatrix}\frac{1}{2ik} & -\frac{1}{2}e^{-ikL}\\ \frac{1}{2ik}e^{-ikL} & \frac{1}{2}\end{bmatrix}\begin{Bmatrix}t(0)\\ u(L)\end{Bmatrix}=\begin{Bmatrix}0\\ 0\end{Bmatrix}, \tag{24}$$

LM equation:

Please cite this article as: Chen JT, et al. On the spurious eigensolutions for the real-part boundary element method. Eng Anal Bound Elem (2008), doi:10.1016/j.enganabound.2008.07.003

$$\begin{bmatrix} \frac{1}{2} & -\frac{ik}{2}e^{-ikL} \\ -\frac{1}{2}e^{-ikL} & -\frac{ik}{2} \end{bmatrix} \begin{Bmatrix} t(0) \\ u(L) \end{Bmatrix} = \begin{Bmatrix} 0 \\ 0 \end{Bmatrix}. \quad (25)$$

Owing to the introduction of degenerate kernels of Eq. (4), dual BIEs for the domain point can be expressed as

$$u(x) = [T(s,x)u(s) - U(s,x)t(s)]\big|_{s=0}^{s=L}, \quad x \in [0,L], \quad (26)$$

$$t(x) = [M(s,x)u(s) - L(s,x)t(s)]\big|_{s=0}^{s=L}, \quad x \in [0,L] \quad (27)$$

and the null-field BIEs is

$$0 = [T(s,x)u(s) - U(s,x)t(s)]\big|_{s=0}^{s=L}, \quad x \in (-\infty,0] \cup [L,\infty), \quad (28)$$

$$0 = [M(s,x)u(s) - L(s,x)t(s)]\big|_{s=0}^{s=L}, \quad x \in (-\infty,0] \cup [L,\infty), \quad (29)$$

where U, T, L and M kernels must be represented in a correct form using the expression of degenerate kernels of Eq. (4). The collocation point can locate on the real boundary two end points for four Eqs. (26)–(29). Mathematically speaking, the domain of Eqs. (26)–(29) is a closed set instead of an open set in the conventional BEM formulation of Eqs. (7) and (8) using the closed-form fundamental solution.

3. Direct-searching scheme for the eigenvalues using seven indicators

According to Eqs. (20)–(25), we use seven determinants to obtain the eigenvalue. Seven indicators to find the eigenvalue by using determinants in the direct-searching scheme are shown below:

Indicator 1: Complex determinant using the complex-valued kernel BEM.
Indicator 2: Absolute value of determinant using the complex-valued kernel BEM.
Indicator 3: Imaginary-part of determinant using the complex-valued kernel BEM.
Indicator 4: Real-part of determinant using the complex-valued kernel BEM.
Indicator 5: Determinant using the imaginary-part kernel BEM.
Indicator 6: Determinant using the real-part kernel BEM.
Indicator 7: Determinant using the MRM [7].

Based on the seven indicators, the true and spurious eigensolutions are shown in Table 3 and the corresponding boundary eigenvectors are summarized in Tables 4–9. Tables 4 and 5 are the results for the case 1 by using *UT* and *LM* equations, respectively, while Tables 6 and 7 are those for the case 2. The results of case 3 are shown in Tables 8 and 9. The first column of each table denotes the indicator for the direct-searching determinant. The second column shows the rank of the influence matrix for the true and spurious eigenvalues. True and spurious eigenvalues are found in the third and sixth columns and their corresponding boundary eigenvectors are listed in the fourth and seventh columns, respectively. Then their analytical solutions are listed in the fifth (true) and eighth (spurious) columns. The last column shows the treatment once the spurious eigenvalue appears.

According to Tables 4–7, for cases 1 and 2, we find that indicator 3 (imaginary part of determinant using the complex-valued kernel) results in spurious eigenvalues. Its treatment is using either the absolute value (indicator 2) or the real-part (indicator 4). For Tables 8 and 9 of the case 3, we find that the indicators 4 and 7 also results in spurious eigenvalues. Since the MRM is nothing but the real-part BEM [7–12], this is the reason why indicators (6) and (7) both result in the same spurious eigenvalue as shown in Tables 8 and 9. We employ the SVD technique in conjunction with the CHEEF idea to suppress the occurrence of spurious eigenvalues as elaborated on later in the next section.

Table 3
Possible eigenequations using seven indicators

		Possible eigenequations
Case 1		
UT	(1)	$\{\sin(kL)\}[\sin(kL)]+i\{\sin(kL)\}[\cos(kL)] = 0$
	(2)	$\{\sin(kL)\} = 0$
	(3)	$\{\sin(kL)\}[\cos(kL)] = 0$
	(4)	$\{\sin(kL)\}[\sin(kL)] = 0$
	(5)	$\{\sin(kL)\}[\sin(kL)] = 0$
	(6) and (7)	$\{\sin(kL)\}[\sin(kL)] = 0$
LM	(1)	$\{\sin(kL)\}[\sin(kL)]+i\{\sin(kL)\}[\cos(kL)] = 0$
	(2)	$\{\sin(kL)\} = 0$
	(3)	$\{\sin(kL)\}[\cos(kL)] = 0$
	(4)	$\{\sin(kL)\}[\sin(kL)] = 0$
	(5)	$\{\sin(kL)\}[\sin(kL)] = 0$
	(6) and (7)	$\{\sin(kL)\}[\sin(kL)] = 0$
Case 2		
UT	(1)	$\{\sin(kL)\}[\sin(kL)]+i\{\sin(kL)\}[\cos(kL)] = 0$
	(2)	$\{\sin(kL)\} = 0$
	(3)	$\{\sin(kL)\}[\cos(kL)] = 0$
	(4)	$\{\sin(kL)\}[\sin(kL)] = 0$
	(5)	$\{\sin(kL)\}[\sin(kL)] = 0$
	(6) and (7)	$\{\sin(kL)\}[\sin(kL)] = 0$
LM	(1)	$\{\sin(kL)\}[\sin(kL)]+i\{\sin(kL)\}[\cos(kL)] = 0$
	(2)	$\{\sin(kL)\} = 0$
	(3)	$\{\sin(kL)\}[\cos(kL)] = 0$
	(4)	$\{\sin(kL)\}[\sin(kL)] = 0$
	(5)	$\{\sin(kL)\}[\sin(kL)] = 0$
	(6) and (7)	$\{\sin(kL)\}[\sin(kL)] = 0$
Case 3		
UT	(1)	$[\sin(kL)]\{\cos(kL)\}+i[\cos(kL)]\{\cos(kL) = 0\}$
	(2)	$\{\cos(kL)\} = 0$
	(3)	$[\cos(kL)]\{\cos(kL)\} = 0$
	(4)	$[\sin(kL)]\{\cos(kL)\} = 0$
	(5)	$[\sin(kL)]\{\cos(kL)\} = 0$
	(6) and (7)	$[\sin(kL)]\{\cos(kL)\} = 0$
LM	(1)	$[\sin(kL)]\{\cos(kL)\}+i[\cos(kL)]\{\cos(kL) = 0\}$
	(2)	$\{\cos(kL)\} = 0$
	(3)	$[\cos(kL)]\{\cos(kL)\} = 0$
	(4)	$[\sin(kL)]\{\cos(kL)\} = 0$
	(5)	$[\sin(kL)]\{\cos(kL)\} = 0$
	(6) and (7)	$[\sin(kL)]\{\cos(kL)\} = 0$

Where the equations inside { } and [ ] denote the true and spurious eigenequations, respectively.

4. SVD technique for filtering out spurious eigenvalues in the real-part BEM by using the CHEEF concept

Because the real-part BEM lacks for the constraining condition of imaginary-part information, spurious eigenvalues appear in the case 3 using the indicator 6 in Tables 8 and 9. In order to filter out spurious eigenvalues, we employ the CHEEF concept and the SVD technique. A point, c, in the complementary domain, which is called a CHEEF point as shown in Figs. 2(a) and (b) is selected to provide a constraint. Therefore we have the null-field equation of case 3 using the indicator 6. The constraints of *UT* and *LM* equations respectively, for the CHEEF point are

$$0 = U_R(0,c)t(0) + T_R(L,c)u(L), \quad c \in (-\infty,0) \cup (L,\infty), \quad (30)$$

$$0 = L_R(0,c)t(0) + M_R(L,c)u(L), \quad c \in (-\infty,0) \cup (L,\infty), \quad (31)$$

where $U_R(0,c)$, $T_R(L,c)$, $L_R(0,c)$ and $M_R(L,c)$ are the real-parts of $U(0,c)$, $T(L,c)$, $L(0,c)$ and $M(L,c)$, respectively. By assembling Eqs.

Table 4
Eigensolutions for the case 1: $u(0)=0$ and $u(l)=0$ (Dirichlet BC) (UT equation) using seven approaches

Rank of $[U(k)]$ (T,S)	True eigenvalue (k_t)	True boundary eigenvector $\begin{Bmatrix} t(0) \\ t(1) \end{Bmatrix}$	True analytical solution $u_t(x)$	Spurious eigenvalue (k_s)	Spurious boundary eigenvector $\begin{Bmatrix} t(0) \\ t(1) \end{Bmatrix}$	Spurious analytical solution $u_s(x)$	Treatment
1 (1,NA)	$\frac{n\pi}{L}$	$\begin{Bmatrix} 1 \\ (-1)^n \end{Bmatrix}$	$\sin\left(\frac{n\pi}{L}x\right)$	NA	NA	NA	NA
2 (1,NA)	$\frac{n\pi}{L}$	$\begin{Bmatrix} 1 \\ (-1)^n \end{Bmatrix}$	$\sin\left(\frac{n\pi}{L}x\right)$	NA	NA	NA	NA
3 (1,2)	$\frac{n\pi}{L}$	$\begin{Bmatrix} 1 \\ (-1)^n \end{Bmatrix}$	$\sin\left(\frac{n\pi}{L}x\right)$	$\frac{(2n-1)}{2L}\pi$	× Rank = 2	× Rank = 2	Taking the absolute value
4 (1,NA)	$\frac{n\pi}{L}$	$\begin{Bmatrix} 1 \\ (-1)^n \end{Bmatrix}$	$\sin\left(\frac{n\pi}{L}x\right)$	NA	NA	NA	NA
5 (1,NA)	$\frac{n\pi}{L}$	$\begin{Bmatrix} 1 \\ (-1)^n \end{Bmatrix}$	× Null equation	NA	NA	NA	NA
6 (0,NA)	$\frac{n\pi}{L}$	× Null matrix	× Null matrix	NA	NA	NA	NA
7 (0,NA)	$\frac{n\pi}{L}$	× Null matrix	× Null matrix	NA	NA	NA	NA

Indicator 3 results in spurious eigensolutions.

Table 5
Eigensolutions for the case 1: $u(0)=0$ and $u(l)=0$ (Dirichlet BC) (LM equation) using seven approaches

Rank of $[U(k)]$ (T,S)	True eigenvalue (k_t)	True boundary eigenvector $\begin{Bmatrix} t(0) \\ t(1) \end{Bmatrix}$	True analytical solution $u_t(x)$	Spurious eigenvalue (k_s)	Spurious boundary eigenvector $\begin{Bmatrix} t(0) \\ t(1) \end{Bmatrix}$	Spurious analytical solution $u_s(x)$	Treatment
1 (1,NA)	$\frac{n\pi}{L}$	$\begin{Bmatrix} 1 \\ (-1)^n \end{Bmatrix}$	$\sin\left(\frac{n\pi}{L}x\right)$	NA	NA	NA	NA
2 (1,NA)	$\frac{n\pi}{L}$	$\begin{Bmatrix} 1 \\ (-1)^n \end{Bmatrix}$	$\sin\left(\frac{n\pi}{L}x\right)$	NA	NA	NA	NA
3 (1,2)	$\frac{n\pi}{L}$	$\begin{Bmatrix} 1 \\ (-1)^n \end{Bmatrix}$	$\sin\left(\frac{n\pi}{L}x\right)$	$\frac{(2n-1)}{2L}\pi$	× Rank = 2	× Rank = 2	Taking the absolute value
4 (1,NA)	$\frac{n\pi}{L}$	$\begin{Bmatrix} 1 \\ (-1)^n \end{Bmatrix}$	$\sin\left(\frac{n\pi}{L}x\right)$	NA	NA	NA	NA
5 (0,NA)	$\frac{n\pi}{L}$	× Null matrix	Null matrix × null equation	NA	NA	NA	NA
6 (1,NA)	$\frac{n\pi}{L}$	$\begin{Bmatrix} 1 \\ (-1)^n \end{Bmatrix}$	$\sin\left(\frac{n\pi}{L}x\right)$	NA	NA	NA	NA
7 (1,NA)	$\frac{n\pi}{L}$	$\begin{Bmatrix} 1 \\ (-1)^n \end{Bmatrix}$	$\sin\left(\frac{n\pi}{L}x\right)$	NA	NA	NA	NA

Indicator 3 results in spurious eigensolutions.

(24) and (30) as well as Eqs. (24) and (31) into the matrix form, and by selecting a right ($c>L$) CHEEF point, we have

UT equation:

$$\begin{bmatrix} 0 & -\frac{\cos(kL)}{2} \\ -\frac{\sin(kL)}{2k} & \frac{1}{2} \\ \frac{\sin(ck)}{2k} & -\frac{\cos[(c-L)k]}{2} \end{bmatrix} \begin{Bmatrix} t(0) \\ u(L) \end{Bmatrix} = \begin{Bmatrix} 0 \\ 0 \\ 0 \end{Bmatrix} \quad (L<c<\infty), \qquad (32)$$

LM equation:

$$\begin{bmatrix} \frac{1}{2} & -\frac{k\sin(kL)}{2} \\ -\frac{\cos(kL)}{2} & 0 \\ \frac{\cos(ck)}{2} & \frac{k\sin[(c-L)k]}{2} \end{bmatrix} \begin{Bmatrix} t(0) \\ u(L) \end{Bmatrix} = \begin{Bmatrix} 0 \\ 0 \\ 0 \end{Bmatrix} \quad (L<c<\infty), \qquad (33)$$

If the CHEEF point c is selected in the left side ($c<0$). We have,

Please cite this article as: Chen JT, et al. On the spurious eigensolutions for the real-part boundary element method. Eng Anal Bound Elem (2008), doi:10.1016/j.enganabound.2008.07.003

Table 6
Eigensolutions for the case 2: $t(0)=0$ and $t(l)=0$ (Neumann BC) (UT equation) using seven approaches

Rank of $[T(k)]$ (T,S)	True eigenvalue (k_t)	True boundary eigenvector $\begin{Bmatrix} u(0) \\ u(1) \end{Bmatrix}$	True analytical solution $u_t(x)$	Spurious eigenvalue (k_s)	Spurious boundary eigenvector $\begin{Bmatrix} u(0) \\ u(1) \end{Bmatrix}$	Spurious analytical solution $u_s(x)$	Treatment
1 (1,NA)	$\frac{n\pi}{L}$	$\begin{Bmatrix} 1 \\ (-1)^n \end{Bmatrix}$	$\cos\left(\frac{n\pi}{L}x\right)$	NA	NA	NA	NA
2 (1,NA)	$\frac{n\pi}{L}$	$\begin{Bmatrix} 1 \\ (-1)^n \end{Bmatrix}$	$\cos\left(\frac{n\pi}{L}x\right)$	NA	NA	NA	NA
3 (1,2)	$\frac{n\pi}{L}$	$\begin{Bmatrix} 1 \\ (-1)^n \end{Bmatrix}$	$\cos\left(\frac{n\pi}{L}x\right)$	$\frac{(2n-1)}{2L}\pi$	× Rank = 2	× Rank = 2	Taking the absolute value
4 (1,NA)	$\frac{n\pi}{L}$	$\begin{Bmatrix} 1 \\ (-1)^n \end{Bmatrix}$	$\cos\left(\frac{n\pi}{L}x\right)$	NA	NA	NA	NA
5 (0,NA)	$\frac{n\pi}{L}$	× Null matrix	Null matrix × null equation	NA	NA	NA	NA
6 (1,NA)	$\frac{n\pi}{L}$	$\begin{Bmatrix} 1 \\ (-1)^n \end{Bmatrix}$	$\cos\left(\frac{n\pi}{L}x\right)$	NA	NA	NA	NA
7 (1,NA)	$\frac{n\pi}{L}$	$\begin{Bmatrix} 1 \\ (-1)^n \end{Bmatrix}$	$\cos\left(\frac{n\pi}{L}x\right)$	NA	NA	NA	NA

Indicator 3 results in spurious eigensolutions.

Table 7
Eigensolutions for the case 2: $t(0)=0$ and $t(l)=0$ (Neumann BC) (LM equation) using seven approaches

Rank of $[T(k)]$ (T,S)	True eigenvalue (k_t)	True boundary eigenvector $\begin{Bmatrix} u(0) \\ u(1) \end{Bmatrix}$	True analytical solution $u_t(x)$	Spurious eigenvalue (k_s)	Spurious boundary eigenvector $\begin{Bmatrix} u(0) \\ u(1) \end{Bmatrix}$	Spurious analytical solution $u_s(x)$	Treatment
1 (1,NA)	$\frac{n\pi}{L}$	$\begin{Bmatrix} 1 \\ (-1)^n \end{Bmatrix}$	$\cos\left(\frac{n\pi}{L}x\right)$	NA	NA	NA	NA
2 (1,NA)	$\frac{n\pi}{L}$	$\begin{Bmatrix} 1 \\ (-1)^n \end{Bmatrix}$	$\cos\left(\frac{n\pi}{L}x\right)$	NA	NA	NA	NA
3 (1,2)	$\frac{n\pi}{L}$	$\begin{Bmatrix} 1 \\ (-1)^n \end{Bmatrix}$	$\cos\left(\frac{n\pi}{L}x\right)$	$\frac{(2n-1)}{2L}\pi$	× Rank = 2	× Rank = 2	Taking the absolute value
4 (1,NA)	$\frac{n\pi}{L}$	$\begin{Bmatrix} 1 \\ (-1)^n \end{Bmatrix}$	$\cos\left(\frac{n\pi}{L}x\right)$	NA	NA	NA	NA
5 (1,NA)	$\frac{n\pi}{L}$	$\begin{Bmatrix} 1 \\ (-1)^n \end{Bmatrix}$	× Null equation	NA	NA	NA	NA
6 (0,NA)	$\frac{n\pi}{L}$	× Null matrix	× Null matrix	NA	NA	NA	NA
7 (0,NA)	$\frac{n\pi}{L}$	× Null matrix	× Null matrix	NA	NA	NA	NA

Indicator 3 results in spurious eigensolutions.

UT equation:

$$\begin{bmatrix} 0 & -\frac{\cos(kL)}{2} \\ -\frac{\sin(kL)}{2k} & \frac{1}{2} \\ -\frac{\sin(ck)}{2k} & \frac{\cos[(c-L)k]}{2} \end{bmatrix} \begin{Bmatrix} t(0) \\ u(L) \end{Bmatrix} = \begin{Bmatrix} 0 \\ 0 \\ 0 \end{Bmatrix} \quad (-\infty < c < 0). \tag{34}$$

LM equation:

$$\begin{bmatrix} \frac{1}{2} & -\frac{k\sin(kL)}{2} \\ -\frac{\cos(kL)}{2} & 0 \\ -\frac{\cos(ck)}{2} & -\frac{k\sin[(c-L)k]}{2} \end{bmatrix} \begin{Bmatrix} t(0) \\ u(L) \end{Bmatrix} = \begin{Bmatrix} 0 \\ 0 \\ 0 \end{Bmatrix} \quad (L < c < \infty), \tag{35}$$

Please cite this article as: Chen JT, et al. On the spurious eigensolutions for the real-part boundary element method. Eng Anal Bound Elem (2008), doi:10.1016/j.enganabound.2008.07.003

Table 8
Eigensolutions for the case 3: $u(0)=0$ and $t(l)=0$ (mixed-type BC) (UT equation) using seven approaches

Rank of $[U(k),T(k)]$ (T,S)	True eigenvalue (k_t)	True boundary eigenvector $\begin{Bmatrix} t(0) \\ u(1) \end{Bmatrix}$	True analytical solution $u_t(x)$	Spurious eigenvalue (k_s)	Spurious boundary eigenvector $\begin{Bmatrix} t(0) \\ u(1) \end{Bmatrix}$	Spurious analytical solution $u_s(x)$	Treatment
1 (1,NA)	$\frac{(2n-1)}{2L}\pi$	$\begin{Bmatrix} \frac{(2n-1)}{2L}\pi \\ (-1)^{n+1} \end{Bmatrix}$	$\sin\left(\frac{(2n-1)\pi x}{2L}\right)$	NA	NA	NA	NA
2 (1,NA)	$\frac{(2n-1)}{2L}\pi$	$\begin{Bmatrix} \frac{(2n-1)}{2L}\pi \\ (-1)^{n+1} \end{Bmatrix}$	$\sin\left(\frac{(2n-1)\pi x}{2L}\right)$	NA	NA	NA	NA
3 (1,NA)	$\frac{(2n-1)}{2L}\pi$	$\begin{Bmatrix} \frac{(2n-1)}{2L}\pi\pi \\ (-1)^{n+1} \end{Bmatrix}$	$\sin\left(\frac{(2n-1)\pi x}{2L}\right)$	NA	NA	NA	NA
4 (1,2)	$\frac{(2n-1)}{2L}\pi$	$\begin{Bmatrix} \frac{(2n-1)}{2L}\pi\pi \\ (-1)^{n+1} \end{Bmatrix}$	$\sin\left(\frac{(2n-1)\pi x}{2L}\right)$	$\frac{n\pi}{L}$	$\times$ Rank = 2	$\times$ Rank = 2	Taking the absolute value
5 (1,1)	$\frac{(2n-1)}{2L}\pi$	$\begin{Bmatrix} \frac{(2n-1)}{2L}\pi\pi \\ (-1)^{n+1} \end{Bmatrix}$	$\times$ Null equation	$\frac{n\pi}{L}$	$\begin{Bmatrix} 0 \\ 1 \end{Bmatrix}$	$\times$ Null equation	CHEEF
6 (1,1)	$\frac{(2n-1)}{2L}\pi$	$\begin{Bmatrix} \frac{(2n-1)}{2L}\pi\pi \\ (-1)^{n+1} \end{Bmatrix}$	$\sin\left(\frac{(2n-1)\pi x}{2L}\right)$	$\frac{n\pi}{L}$	$\begin{Bmatrix} 0 \\ 1 \end{Bmatrix}$	$\sin\left(\frac{n\pi}{L}x\right)$	CHEEF
7 (1,1)	$\frac{(2n-1)}{2L}\pi$	$\begin{Bmatrix} \frac{(2n-1)}{2L}\pi\pi \\ (-1)^{n+1} \end{Bmatrix}$	$\sin\left(\frac{(2n-1)\pi x}{2L}\right)$	$\frac{n\pi}{L}$	$\begin{Bmatrix} 0 \\ 1 \end{Bmatrix}$	$\sin\left(\frac{n\pi}{L}x\right)$	CHEEF

Indicators 4–7 result in spurious eigensolutions.

Table 9
Eigensolutions for the case 3: $u(0)=0$ and $t(l)=0$ (mixed-type BC) (LM equation) using seven approaches

Rank of $[L(k),M(k)]$ (T,S)	True eigenvalue (k_t)	True boundary eigenvector $\begin{Bmatrix} t(0) \\ u(1) \end{Bmatrix}$	True analytical solution $u_t(x)$	Spurious eigenvalue (k_s)	Spurious boundary eigenvector $\begin{Bmatrix} t(0) \\ u(1) \end{Bmatrix}$	Spurious analytical solution $u_s(x)$	Treatment
1 (1,NA)	$\frac{(2n-1)}{2L}\pi$	$\begin{Bmatrix} \frac{(2n-1)}{2L}\pi \\ (-1)^{n+1} \end{Bmatrix}$	$\sin\left(\frac{(2n-1)\pi x}{2L}\right)$	NA	NA	NA	NA
2 (1,NA)	$\frac{(2n-1)}{2L}\pi$	$\begin{Bmatrix} \frac{(2n-1)}{2L}\pi \\ (-1)^{n+1} \end{Bmatrix}$	$\sin\left(\frac{(2n-1)\pi x}{2L}\right)$	NA	NA	NA	NA
3 (1,NA)	$\frac{(2n-1)}{2L}\pi$	$\begin{Bmatrix} \frac{(2n-1)}{2L}\pi \\ (-1)^{n+1} \end{Bmatrix}$	$\sin\left(\frac{(2n-1)\pi x}{2L}\right)$	NA	NA	NA	NA
4 (1,2)	$\frac{(2n-1)}{2L}\pi$	$\begin{Bmatrix} \frac{(2n-1)}{2L}\pi \\ (-1)^{n+1} \end{Bmatrix}$	$\sin\left(\frac{(2n-1)\pi x}{2L}\right)$	$\frac{n\pi}{L}$	$\times$ Rank = 2	$\times$ Rank = 2	Taking the absolute value
5 (1,1)	$\frac{(2n-1)}{2L}\pi$	$\begin{Bmatrix} \frac{(2n-1)}{2L}\pi \\ (-1)^{n+1} \end{Bmatrix}$	$\times$ Null equation	$\frac{n\pi}{L}$	$\begin{Bmatrix} 0 \\ 1 \end{Bmatrix}$	$\times$ Null equation	CHEEF
6 (1,1)	$\frac{(2n-1)}{2L}\pi$	$\begin{Bmatrix} \frac{(2n-1)}{2L}\pi \\ (-1)^{n+1} \end{Bmatrix}$	$\sin\left(\frac{(2n-1)\pi x}{2L}\right)$	$\frac{n\pi}{L}$	$\begin{Bmatrix} 0 \\ 1 \end{Bmatrix}$	$\cos\left(\frac{n\pi}{L}x\right)$	CHEEF
7 (1,1)	$\frac{(2n-1)}{2L}\pi$	$\begin{Bmatrix} \frac{(2n-1)}{2L}\pi \\ (-1)^{n+1} \end{Bmatrix}$	$\sin\left(\frac{(2n-1)\pi x}{2L}\right)$	$\frac{n\pi}{L}$	$\begin{Bmatrix} 0 \\ 1 \end{Bmatrix}$	$\cos\left(\frac{n\pi}{L}x\right)$	CHEEF

Indicators 4–7 result in spurious eigensolutions.

Please cite this article as: Chen JT, et al. On the spurious eigensolutions for the real-part boundary element method. Eng Anal Bound Elem (2008), doi:10.1016/j.enganabound.2008.07.003

It is interesting to find that the left $(-\infty<c<0)$ and right $(L<c<\infty)$ CHEEF points yield the same row but negative to each other due to the CHEEF point as shown in Eqs. (32)–(35).

Based on the SVD technique, we have

$$[K]=[\Phi][\Sigma][\Psi]^{\mathrm{T}}, \tag{36}$$

where $[K]$ is the influence matrix in Eqs. (32)–(35), $[\Phi]$ is a left unitary matrix constructed by the left singular vectors (ϕ_1,ϕ_2,ϕ_3),

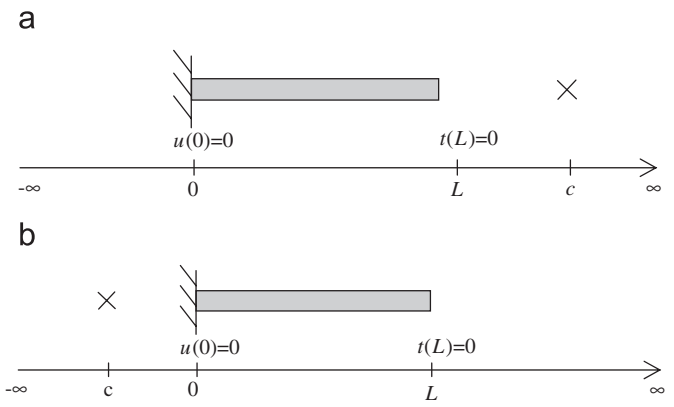

Fig. 2. (a) A CHEEF point, c, in the right side of case 3 ($c>L$) and (b) a CHEEF point, c, in the left side of case 3 ($c<0$).

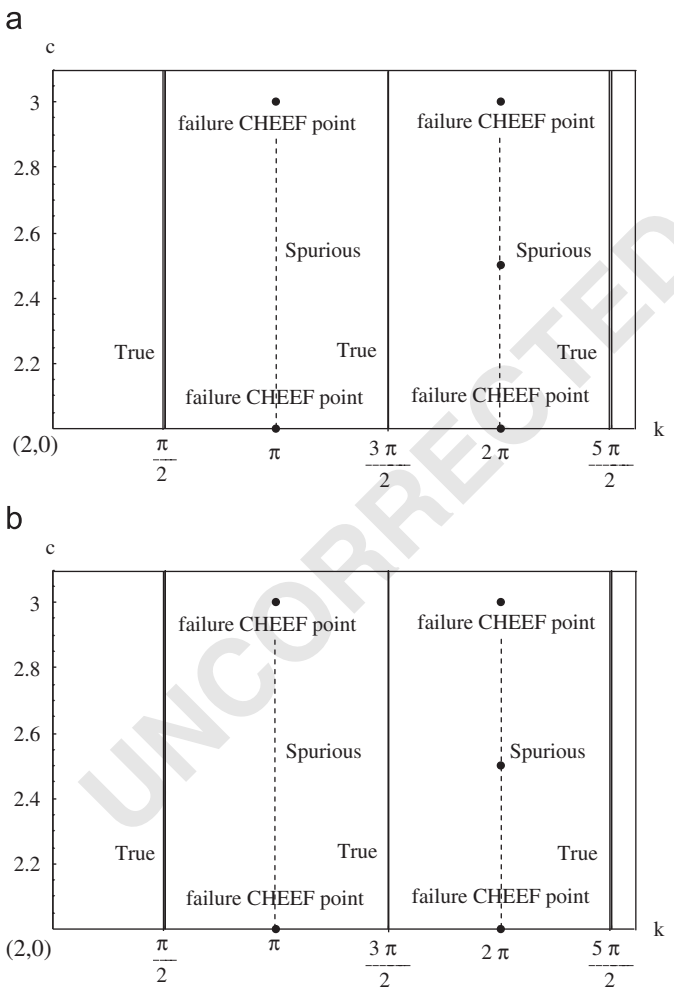

Fig. 3. (a) Contour plot of the minimum singular value σ_1 versus (k,c) by using the UT equation (zero nodal line only) and (b) contour plot of the minimum singular value σ_1 versus (k,c) by using the LM equation (zero nodal line only).

$[\Sigma]$ is a diagonal matrix which has singular values σ_1 and σ_2 allocated in a diagonal line as

$$[\Sigma]=\begin{bmatrix}\sigma_2 & 0\\ 0 & \sigma_1\\ 0 & 0\end{bmatrix}, \tag{37}$$

in which $\sigma_2\geqslant\sigma_1$, σ_2 and σ_1 are the functions of c, k and L, and $[\Psi]^{\mathrm{T}}$ is the transpositional matrix of a right unitary matrix constructed by the right singular vectors (ψ_1,ψ_2). As we can see in Eq. (37), there exist at most 2 nonzero singular values. The rank of influence matrices are equal to 2 at most. Since the boundary eigenvector is nontrivial, the rank of influence matrices must be one. Therefore the minimum singular value σ_1 must be zero.

We show two contour figures of case 3 for σ_1 versus (k,c) by using the *UT* and the *LM* equations that are shown in Figs. 3(a) and (b). The length L of a rod is 1. The k-axis is the wave number and the c-axis is the location of CHEEF point in Figs. 3(a) and (b). It is found that no matter what value c is, σ_1 is always zero for the true eigenvalue of $k_T=((2n-1)/2L)\pi$, $n\in N$. For the spurious eigenvalue of $k_S=n\pi/L$, $n\in N$, failure CHEEF points appear when $kc=n\pi$, $n\in N$. Since the CHEEF constraint is trivial which cannot filter out spurious eigenvalues. True and spurious modes of the case 3 by using the *UT* equation are shown in Figs. 4 and 5, respectively. It indicates that a true eigenvalue results in a true mode in the domain and null field in the complementary domain, while the spurious case has a nontrivial field in the complementary domain. The location of zero response in the complementary domain happens to be that of the failure CHEEF point.

5. Updating terms and updating documents to extract out true and spurious eigenvalues

Now we arrange Eqs. (18) and (19) for the case 3 by using the indicator 6, we have

$$[A]\begin{Bmatrix}t(0)\\ u(L)\end{Bmatrix}=[B]\begin{Bmatrix}u(0)\\ t(L)\end{Bmatrix}, \tag{38}$$

$$[C]\begin{Bmatrix}t(0)\\ u(L)\end{Bmatrix}=[D]\begin{Bmatrix}u(0)\\ t(L)\end{Bmatrix}, \tag{39}$$

where $[A]$, $[B]$, $[C]$ and $[D]$ are influence matrices of Eqs. (18) and (19), and can be shown below:

$$[A]=\begin{bmatrix}0 & -\frac{1}{2}\cos(kL)\\ -\frac{1}{2k}\sin(kL) & \frac{1}{2}\end{bmatrix}, \tag{40}$$

$$[B]=\begin{bmatrix}-\frac{1}{2} & -\frac{1}{2k}\sin(kL)\\ \frac{1}{2}\cos(kL) & 0\end{bmatrix}, \tag{41}$$

$$[C]=\begin{bmatrix}\frac{1}{2} & -\frac{k}{2}\sin(kL)\\ -\frac{1}{2}\cos(kL) & 0\end{bmatrix}, \tag{42}$$

$$[D]=\begin{bmatrix}0 & \frac{1}{2}\cos(kL)\\ -\frac{k}{2}\sin(kL) & -\frac{1}{2}\end{bmatrix}. \tag{43}$$

In order to extract out true and spurious eigenvalues, we utilize updating terms and updating documents, respectively. Therefore, we combine $[A]$ with $[C]$ and $[A]$ with $[B]$, which can be written as

Please cite this article as: Chen JT, et al. On the spurious eigensolutions for the real-part boundary element method. Eng Anal Bound Elem (2008), doi:10.1016/j.enganabound.2008.07.003

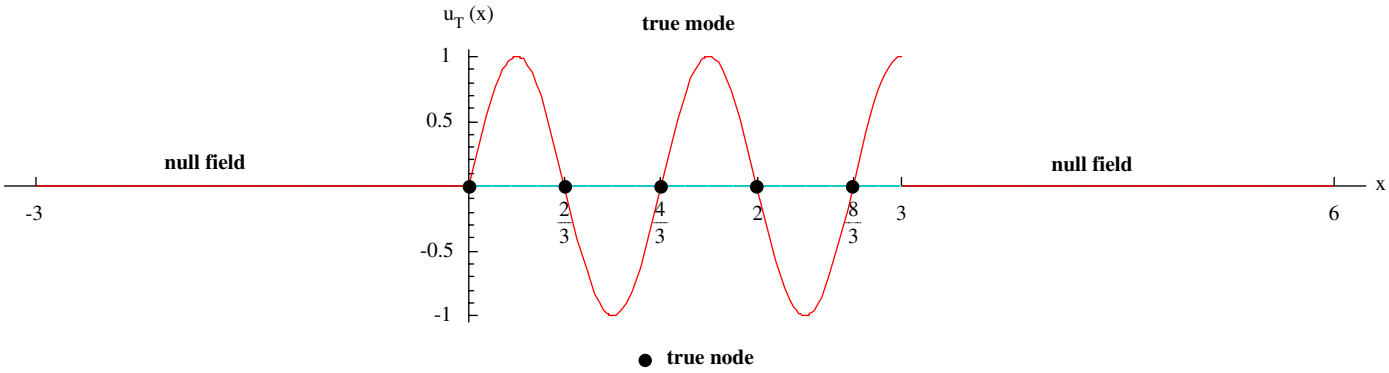

Fig. 4. True mode of case 3 by using the UT equation ($k_T = 4.5\pi$, $L = 3$).

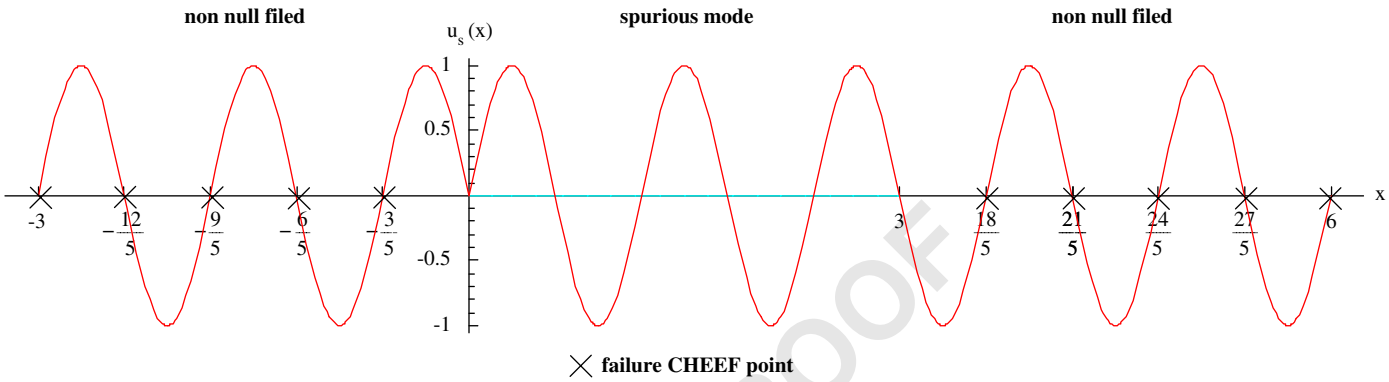

Fig. 5. Spurious mode of case 3 by using the UT equation ($k_S = 5\pi$, $L = 3$).

$$\begin{bmatrix} A \\ C \end{bmatrix} = \begin{bmatrix} 0 & -\frac{1}{2}\cos(kL) \\ -\frac{1}{2k}\sin(kL) & \frac{1}{2} \\ \frac{1}{2} & -\frac{k}{2}\sin(kL) \\ -\frac{1}{2}\cos(kL) & 0 \end{bmatrix}, \tag{44}$$

$$\begin{bmatrix} A & B \end{bmatrix} = \begin{bmatrix} 0 & -\frac{1}{2}\cos(kL) & -\frac{1}{2} & -\frac{1}{2k}\sin(kL) \\ -\frac{1}{2k}\sin(kL) & \frac{1}{2} & \frac{1}{2}\cos(kL) & 0 \end{bmatrix}. \tag{45}$$

By employing SVD for $\begin{bmatrix} A \\ C \end{bmatrix}$ and $\begin{bmatrix} A & B \end{bmatrix}$, respectively, the minimum singular values versus k can be obtained. The figures of minimum singular values versus k are shown in Figs. 6(a) and (b) for the unit length rod. The k-value at drops in Figs. 6(a) and (b) show the true and spurious eigenvalues, respectively.

It is interesting that the SVD structure for the four influence matrices are shown in Table 10. We find that the common ϕ and ψ exist for the true and spurious eigenvalues such that

$$\begin{bmatrix} A \\ C \end{bmatrix} \underset{\sim}{\psi} = \underset{\sim}{0}, \quad k = k_T, \tag{46}$$

$$\begin{bmatrix} B \\ D \end{bmatrix} \underset{\sim}{\psi} = \underset{\sim}{0}, \quad k = k_T, \tag{47}$$

$$\underset{\sim}{\phi}^{\mathrm{T}} \begin{bmatrix} A & B \end{bmatrix} = \underset{\sim}{0}, \quad k = k_S, \tag{48}$$

$$\underset{\sim}{\phi}^{\mathrm{T}} \begin{bmatrix} C & D \end{bmatrix} = \underset{\sim}{0}, \quad k = k_S. \tag{49}$$

6. Extension to 2-D and 3-D eigenproblems

Following the simple example of 1-D rod, it is straightforward to extend 2-D and 3-D cases as shown in Figs. 7(a)–(c). The degenerate kernels in Eq. (4) for the 2-D circular case here is

$$U(s,x) = \begin{cases} U^i(s,x) = -\dfrac{\pi i}{2}\sum\limits_{m=0}^{\infty} \varepsilon_m J_m(k\rho) H_m^{(1)}(kR)\cos(m(\theta-\phi)), & R \geqslant \rho, \\ U^e(s,x) = -\dfrac{\pi i}{2}\sum\limits_{m=0}^{\infty} \varepsilon_m H_m^{(1)}(k\rho) J_m(kR)\cos(m(\theta-\phi)), & \rho > R, \end{cases} \tag{50}$$

where $x = (\rho,\phi)$ and $s = (R,\theta)$, J_m and $H_m^{(1)}$ are the mth order cylindrical Bessel function and the cylindrical Hankel function of the first kind, respectively, the superscripts "i" and "e" denote the interior and exterior cases for the kernel expressions, respectively, and ε_m is the Neumann factor

$$\varepsilon_m = \begin{cases} 1, & m = 0, \\ 2, & m = 1,2,\ldots,\infty. \end{cases} \tag{51}$$

For the three-dimensional spherical case, the degenerate kernel is shown below

Please cite this article as: Chen JT, et al. On the spurious eigensolutions for the real-part boundary element method. Eng Anal Bound Elem (2008), doi:10.1016/j.enganabound.2008.07.003

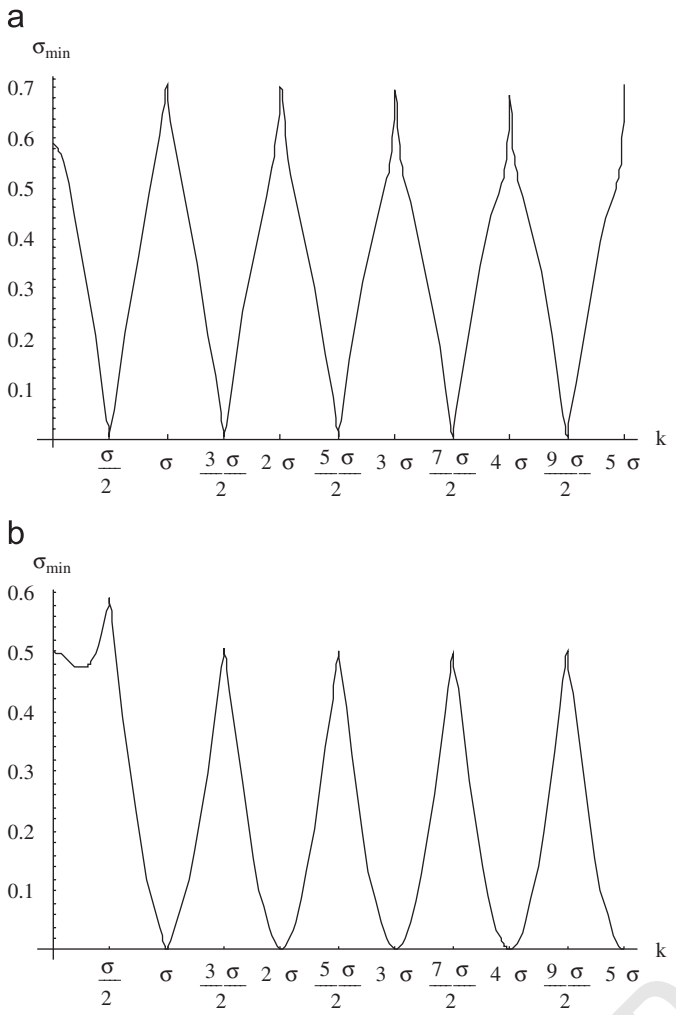

Fig. 6. (a) Extraction of true eigenvalue using SVD updating terms and (b) extraction of spurious eigenvalue using SVD updating documents.

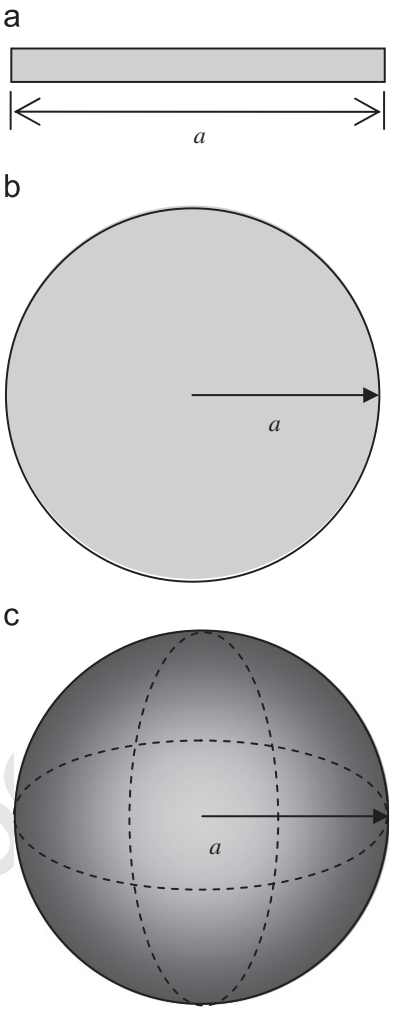

Fig. 7. (a) One-dimensional case (rod), (b) two-dimensional case (circle membrane) and (c) three-dimensional case (spherical cavity).

Table 10
The SVD structure of the four influence matrices for a rod in the dual BEM

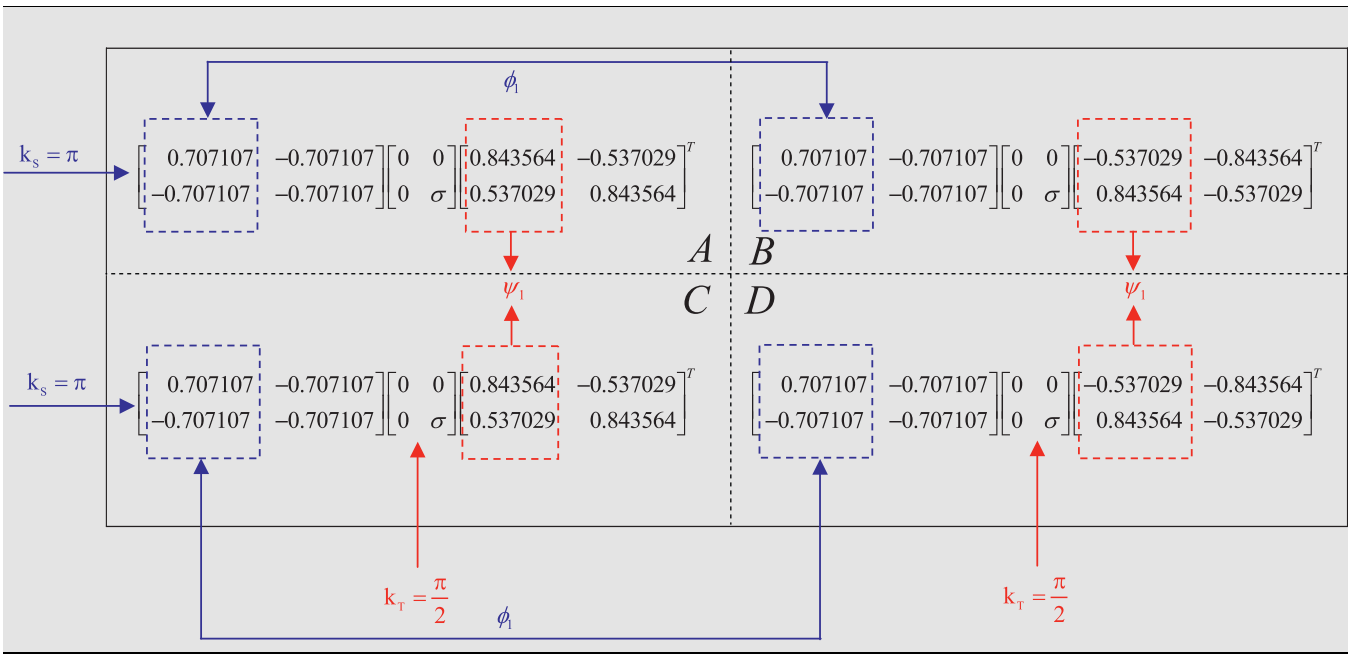

Table 11
Determinants for the 2-D circular membrane subject to the Dirichlet BC

Equation Exact sol.	*UT* $J_n(ka)=0$	*LM* $J_n(ka)=0$
Indicator 1 Det[*C*]	$\pi^{4n}a^{2n}J_0(J_1\dots J_{n-1})^2J_nq_0(q_1\dots q_{n-1})^2 \times q_n\,e^{i(\theta_0+2\sum_{k=1}^{n-1}\theta_k+\theta_n)}=0$	$\pi^{4n}k^{2n}a^{2n}J_0(J_1\dots J_{n-1})^2J_np_0(p_1\dots p_{n-1})^2 \times p_n\,e^{i(\omega_0+2\sum_{k=1}^{n-1}\omega_k+\omega_n)}=0$
Indicator 2 Abs{det[*C*]}	$\pi^{4n}a^{2n}J_0(J_1\dots J_{n-1})^2J_nq_0(q_1\dots q_{n-1})^2q_n=0$	$\pi^{4n}k^{2n}a^{2n}J_0(J_1\dots J_{n-1})^2J_np_0(p_1\dots p_{n-1})^2p_n=0$
Indicator 3 Im{det[*C*]}	$\pi^{4n}a^{2n}J_0(J_1\dots J_{n-1})^2J_nq_0(q_1\dots q_{n-1})^2 \times q_n\,\sin(\theta_0+2\sum_{k=1}^{n-1}\theta_k+\theta_n)=0$	$\pi^{4n}k^{2n}a^{2n}J_0(J_1\dots J_{n-1})^2J_np_0(p_1\dots p_{n-1})^2 \times p_n\,\sin(\omega_0+2\sum_{k=1}^{n-1}\omega_k+\omega_n)=0$
Indicator 4 Re{det[*C*]}	$\pi^{4n}a^{2n}J_0(J_1\dots J_{n-1})^2J_nq_0(q_1\dots q_{n-1})^2 \times q_n\,\cos(\theta_0+2\sum_{k=1}^{n-1}\theta_k+\theta_n)=0$	$\pi^{4n}k^{2n}a^{2n}J_0(J_1\dots J_{n-1})^2J_np_0(p_1\dots p_{n-1})^2 \times p_n\,\cos(\omega_0+2\sum_{k=1}^{n-1}\omega_k+\omega_n)=0$
Indicator 5 det[*I*]	$J_0J_0(J_1J_1J_2J_2\dots J_{n-1}J_{n-1})^2J_nY_n=0$	$J_0J'_0(J_1J'_1J_2J'_2\dots J_{n-1}J'_{n-1})^2J_nY_n=0$
Indicator 6 det[*R*]	$J_0Y_0(J_1Y_1J_2Y_2\dots J_{n-1}Y_{n-1})^2J_nY_n=0$	$J_0Y'_0(J_1Y'_1J_2Y'_2\dots J_{n-1}Y'_{n-1})^2J_nY_n=0$

where Y_n is the nth order Bessel function of the second kind, $q_n=\sqrt{J_n^2+Y_n^2}$, $\theta_n=\tan^{-1}(Y_n/J_n)$, $p_n=\sqrt{J'^2_n+Y'^2_n}$, and $\omega_n=\tan^{-1}(Y'_n/J'_n)$.

Table 12
Determinants for the 2-D circular membrane subject to the Neumann BC

Equation Exact sol.	*UT* $J'_n(ka)=0$	*LM* $J'_n(ka)=0$
Indicator 1 Det[*C*]	$\pi^{4n}k^{2n}a^{2n}J'_0(J'_1\dots J'_{n-1})^2J'_nq_0(q_1\dots q_{n-1})^2 \times q_n\,e^{i(\theta_0+2\sum_{k=1}^{n-1}\theta_k+\theta_n)}=0$	$\pi^{4n}k^{4n}a^{2n}J'_0(J'_1\dots J'_{n-1})^2J'_np_0(p_1\dots p_{n-1})^2 \times p_n\,e^{i(\omega_0+2\sum_{k=1}^{n-1}\omega_k+\omega_n)}=0$
Indicator 2 Abs{det[*C*]}	$\pi^{4n}k^{2n}a^{2n}J'_0(J'_1\dots J'_{n-1})^2J'_nq_0(q_1\dots q_{n-1})^2q_n=0$	$\pi^{4n}k^{4n}a^{2n}J'_0(J'_1\dots J'_{n-1})^2J'_np_0(p_1\dots p_{n-1})^2p_n=0$
Indicator 3 Im{det[*C*]}	$\pi^{4n}k^{2n}a^{2n}J'_0(J'_1\dots J'_{n-1})^2J'_nq_0(q_1\dots q_{n-1})^2 \times q_n\,\sin(\theta_0+2\sum_{k=1}^{n-1}\theta_k+\theta_n)=0$	$\pi^{4n}k^{4n}a^{2n}J'_0(J'_1\dots J'_{n-1})^2J'_np_0(p_1\dots p_{n-1})^2 \times p_n\,\sin(\omega_0+2\sum_{k=1}^{n-1}\omega_k+\omega_n)=0$
Indicator 4 Re{det[*C*]}	$\pi^{4n}k^{2n}a^{2n}J'_0(J'_1\dots J'_{n-1})^2J'_nq_0(q_1\dots q_{n-1})^2 \times q_n\,\cos(\theta_0+2\sum_{k=1}^{n-1}\theta_k+\theta_n)=0$	$\pi^{4n}k^{4n}a^{2n}J'_0(J'_1\dots J'_{n-1})^2J'_np_0(p_1\dots p_{n-1})^2 \times p_n\,\cos(\omega_0+2\sum_{k=1}^{n-1}\omega_k+\omega_n)=0$
Indicator 5 det[*I*]	$J_0J'_0(J_1J'_1J_2J'_2\dots J_{n-1}J'_{n-1})^2J_nY_n=0$	$J'_0J'_0(J'_1J'_1J_2J'_2\dots J'_{n-1}J'_{n-1})^2J_nY_n=0$
Indicator 6 det[*R*]	$J'_0Y_0(J'_1Y_1J'_2Y_2\dots J'_{n-1}Y_{n-1})^2J_nY_n=0$	$J'_0Y'_0(J'_1Y'_1J'_2Y'_2\dots J'_{n-1}Y'_{n-1})^2J_nY_n=0$

Where $q_n=\sqrt{J_n^2+Y_n^2}$, $\theta_n=\tan^{-1}(Y_n/J_n)$, $p_n=\sqrt{J'^2_n+Y'^2_n}$, and $\omega_n=\tan^{-1}(Y'_n/J'_n)$.

Table 13
Eigenequations for the 2-D circular membrane subject to the Dirichlet BC

Equation Exact sol.	*UT* *J*		*LM* *J*	
	True	Spurious	True	Spurious
Indicator 2 Abs{det[*C*]}	$J_0(J_1\dots J_{n-1})^2J_n$	None	$J_0(J_1\dots J_{n-1})^2J_n$	None
Indicator 3 Im{det[*C*]}	$J_0(J_1\dots J_{n-1})^2J_n$	$\sin(\theta_0+2\sum_{k=1}^{n-1}\theta_k+\theta_n)$	$J_0(J_1\dots J_{n-1})^2J_n$	$\sin(\omega_0+2\sum_{k=1}^{n-1}\omega_k+\omega_n)$
Indicator 4 Re{det[*C*]}	$J_0(J_1\dots J_{n-1})^2J_n$	$\cos(\theta_0+2\sum_{k=1}^{n-1}\theta_k+\theta_n)$	$J_0(J_1\dots J_{n-1})^2J_n$	$\cos(\omega_0+2\sum_{k=1}^{n-1}\omega_k+\omega_n)$

Please cite this article as: Chen JT, et al. On the spurious eigensolutions for the real-part boundary element method. Eng Anal Bound Elem (2008), doi:10.1016/j.enganabound.2008.07.003

Table 13 (*continued*)

Equation Exact sol.	*UT* *J*		*LM* *J*	
	True	Spurious	True	Spurious
Indicator 5 det[*I*]	$J_i,\quad i=1,2\ldots n$	$J_i,\quad i=1,2\ldots n$	$J_i,\quad i=1,2\ldots n$	$J'_i,\quad i=1,2\ldots n$
Indicator 6 det[*R*]	$J_i,\quad i=1,2\ldots n$	$Y_i,\quad i=1,2\ldots n$	$J_i,\quad i=1,2\ldots n$	$J'_i,\quad i=1,2\ldots n$

Where $q_n=\sqrt{J_n^2+Y_n^2}$, $\theta_n=\tan^{-1}(Y_n/J_n)$, , $p_n=\sqrt{J'^2_n+Y'^2_n}$, and $\omega_n=\tan^{-1}(Y'_n/J'_n)$.

Table 14
Eigenequations for the 2-D circular membrane subject to the Neumann BC

Equation Exact sol.	*UT* *J′*		*LM* *J′*	
	True	Spurious	True	Spurious
Indicator 2 Abs{det[*C*]}	$J'_0(J'_1\ldots J'_{n-1})^2J'_n$	None	$J'_0(J'_1\ldots J'_{n-1})^2J'_n$	None
Indicator 3 Im{det[*C*]}	$J'_0(J'_1\ldots J'_{n-1})^2J'_n$	$\sin(\theta_0+2\sum_{k=1}^{n-1}\theta_k+\theta_n)$	$J'_0(J'_1\ldots J'_{n-1})^2J'_n$	$\sin(\omega_0+2\sum_{k=1}^{n-1}\omega_k+\omega_n)$
Indicator 4 Re{det[*C*]}	$J'_0(J'_1\ldots J'_{n-1})^2J'_n$	$\cos(\theta_0+2\sum_{k=1}^{n-1}\theta_k+\theta_n)$	$J'_0(J'_1\ldots J'_{n-1})^2J'_n$	$\cos(\omega_0+2\sum_{k=1}^{n-1}\omega_k+\omega_n)$
Indicator 5 det[*I*]	$J'_i,\quad i=1,2\ldots n$	$J_i,\quad i=1,2\ldots n$	$J'_i,\quad i=1,2\ldots n$	$J'_i,\quad i=1,2\ldots n$
Indicator 6 det[*R*]	$J'_i,\quad i=1,2\ldots n$	$Y_i,\quad i=1,2\ldots n$	$J'_i,\quad i=1,2\ldots n$	$Y'_i,\quad i=1,2\ldots n$

Where $q_n=\sqrt{J_n^2+Y_n^2}$, $\theta_n=\tan^{-1}(Y_n/J_n)$, $p_n=\sqrt{J'^2_n+Y'^2_n}$, and $\omega_n=\tan^{-1}(Y'_n/J'_n)$.

Table 15(a)
Occurring mechanism of 1-D true and spurious eigenequations by using the real-part and imaginary-part BEMs

	Dirichlet	Neumann	Mixed-type
UT (imaginary-part)	$\{\sin(kL)\}[\sin(kL)]=0$	$\{\sin(kL)\}[\sin(kL)]=0$	$\{\cos(k)\}[\sin(k)]=0$
LM (imaginary-part)	$\{\sin(kL)\}[\sin(kL)]=0$	$\{\sin(kL)\}[\sin(kL)]=0$	$\{\cos(k)\}[\sin(k)]=0$
UT (real-part)	$\{\sin(kL)\}[\sin(kL)]=0$	$\{\sin(kL)\}[\sin(kL)]=0$	$\{\cos(k)\}[\sin(k)]=0$
LM (real-part)	$\{\sin(kL)\}[\sin(kL)]=0$	$\{\sin(kL)\}[\sin(kL)]=0$	$\{\cos(k)\}[\sin(k)]=0$

Where the equations inside { } and [ ] denote the true and spurious eigenequations, respectively.

$$U(s,x)=\begin{cases} U^i=\mathrm{i}k\sum_{n=0}^{\infty}(2n+1)\sum_{m=0}^{n}\varepsilon_m\frac{(n-m)!}{(n+m)!}\cos[m(\phi-\bar{\phi})] \\ \quad\times P_n^m(\cos\theta)P_n^m(\cos\bar{\theta})j_n(k\rho)h_n^{(2)}(k\bar{\rho}),\quad \bar{\rho}>\rho, \\ U^e=\mathrm{i}k\sum_{n=0}^{\infty}(2n+1)\sum_{m=0}^{n}\varepsilon_m\frac{(n-m)!}{(n+m)!}\cos[m(\phi-\bar{\phi})] \\ \quad\times P_n^m(\cos\theta)P_n^m(\cos\bar{\theta})j_n(k\bar{\rho})h_n^{(2)}(k\rho),\quad \rho>\bar{\rho}, \end{cases} \tag{52}$$

where $x=(\rho,\phi,\theta)$ and $s=(\bar{\rho},\bar{\phi},\bar{\theta})$, j_n and $h_n^{(2)}$ are the nth order spherical Bessel function of the first kind and the nth order spherical Hankel function of the second kind, respectively, and P_n^m is the associated Lengendre polynomial. By extending the boundary densities of $u(0)$, $u(L)$, $t(0)$ and $t(L)$ for the 1-D case to 2-D and 3-D cases, we have

$$u(\theta)=\sum_{n=0}^{\infty}[a_n\cos(n\theta)+b_n\sin(n\theta)], \tag{53}$$

$$t(\theta)=\sum_{n=0}^{\infty}[p_n\cos(n\theta)+q_n\sin(n\theta)], \tag{54}$$

for the 2-D case, and

$$u(\theta,\phi)=\sum_{n=0}^{\infty}\sum_{m=0}^{\infty}u_{mn}P_n^m[\cos(\theta)][\cos(m\phi)], \tag{55}$$

$$t(\theta,\phi)=\sum_{n=0}^{\infty}\sum_{m=0}^{\infty}t_{mn}P_n^m[\cos(\theta)][\cos(m\phi)], \tag{56}$$

for the three-dimensional case, where a_n, b_n, p_n and q_n are Fourier coefficients, u_{mn} and t_{mn} are unknown spherical coefficients.

Following the success of 1-D experience, true and spurious eigensolutions using the six indicators for the 2-D cases are shown in Tables 11–14. Tables 11 and 13 are for the results of Dirichlet problem, while Tables 12 and 14 show those of Neumann problem. The former two tables show the determinants using six indicators, the latter two give the eigensolution. It also indicates that spurious eigensolution occurs for both cases (Dirichlet and

Please cite this article as: Chen JT, et al. On the spurious eigensolutions for the real-part boundary element method. Eng Anal Bound Elem (2008), doi:10.1016/j.enganabound.2008.07.003

Table 15(b)
Occurring mechanism of 2-D true and spurious eigenequations by using the real-part and imaginary-part BEMs

	Dirichlet	Neumann
UT (imaginary-part)	$\{J\}[J]=0$	$\{J'\}[J]=0$
LM (imaginary-part)	$\{J\}[J']=0$	$\{J'\}[J']=0$
UT (real-part)	$\{J\}[Y]=0$	$\{J'\}[Y]=0$
LM (real-part)	$\{J\}[Y']=0$	$\{J'\}[Y']=0$

Where the equations inside { } and [ ] denote the true and spurious eigenequations, respectively.

Table 15(c)
Occurring mechanism of 3-D true and spurious eigenequations by using the real-part and imaginary-part BEMs

	Dirichlet	Neumann
UT (imaginary-part)	$\{j\}[j]=0$	$\{j'\}[j]=0$
LM (imaginary-part)	$\{j\}[j']=0$	$\{j'\}[j']=0$
UT (real-part)	$\{j\}[y]=0$	$\{j'\}[y]=0$
LM (real-part)	$\{j\}[y']=0$	$\{j'\}[y']=0$

Where the equations inside { } and [ ] denote the true and spurious eigenequations, respectively.

Table 16
Hilbert transform pair for the frequency-domain fundamental solutions

Real	Imaginary
$\cos(kr)$	$\sin(kr)$
$J_0(kr)$	$Y_0(kr)$
$\dfrac{\sin(kr)}{r}$	$\dfrac{1-\cos(kr)}{r}$

Neumann) when only real-part kernel is used. True and spurious eigenequations for 1-D rod, 2-D circle and 3-D sphere are summarized in Tables 15(a)–(c), once the real-part BEM is employed. It is interesting to find that only sine and cosine functions occur in the 1-D case of Table 15(a), while J, Y, J', Y' and j, y, j', y' appear for the 2-D and 3-D cases of Tables 15(b) and (c). The reason is that cosine and sine are not only the Hilbert transform pair but they are also differentiation pair. Also the J_0 and Y_0 are the Hilbert transform pair. For the three-dimensional case, we have $\cos(kr)/r$ and $\sin(kr)/r$ as the Hilbert transform pair. The Hilbert transform pairs in Table 16 follow from the requirement of causal effect in the time-domain. Since the frequency-domain fundamental solution is the Fourier transform of time-domain fundamental solution, the causal function in the time-domain implies the Hilbert transform pair in the frequency domain. Therefore, using the complex-valued kernel seems uneconomical. This is the reason why the real-part BEM by adding one CHEEF point can save the computation time.

7. Conclusions

A simple example of 1-D eigenproblem was demonstrated to show that seven indicators of determinant by using the direct-searching scheme can obtain the possible solution. Spurious eigensolutions in the real-part BEM as well as the MRM have been studied analytically. The CHEEF concept in conjunction with the SVD updating technique was applied to filter out spurious eigenvalues. Possible failure points were also examined. Also, the four influence matrices in the dual BEM were all decomposed into SVD form. Common true and spurious eigenvectors were found in the unitary vectors of four matrices. It is interesting that true and spurious eigenvectors are imbedded in the right and left unitary vectors in the SVD, respectively. Extensions to 2-D and 3-D cases were also made. The Hilbert transform pair for the real and imaginary kernel was also examined. The sequence of 1-D examples gives a real good insight in the topic of spurious eigensolutions.

Uncited reference

[37].

Acknowledgement

The financial support (July–October, 2007) from the National Taiwan Ocean University to the undergraduate student (J.W.L.) is gratefully acknowledged.

References

[1] Ali A, Rajakumar C, Yunus SM. Advances in acoustic eigenvalue analysis using boundary element method. Comput Struct 1995;56(5):837–47.
[2] Winkler JR, Davies JB. Elimination of spurious modes in finite element analysis. J Comput Phys 1984;56:1–14.
[3] Greenberg MD. Advanced engineering mathematics, 2nd ed.. New York: Prentice-Hall; 1998.
[4] Fujiwara H. High-accurate numerical computation with multiple-precision arithmetic and spectral method, 2006, private communication.
[5] Zhao S. On the spurious solutions in the high-order finite difference methods for eigenvalue problems. Comput Methods Appl Mech Eng 2007;196:5031–46.
[6] Kuo SR, Chen JT, Huang CX. Analytical study and numerical experiments for true and spurious eigensolutions of a circular cavity using the real-part dual BEM. Int J Numer Methods Eng 2000;48:1401–22.
[7] Chen JT, Wong FC. Analytical derivations for one-dimensional eigenproblems using dual boundary element method and multiple reciprocity method. Eng Anal Bound Elem 1997;20:25–33.
[8] Chen JT, Wong FC. Dual formulation of multiple reciprocity method for the acoustic mode of a cavity with a thin partition. J Sound Vib 1998;217(1):75–95.
[9] Yeih W, Chen JT, Chen KH, Wong FC. A study on the multiple reciprocity method and complex-valued formulation for the Helmholtz equation. Adv Eng Software 1998;29(1):1–6.
[10] Yeih W, Chen JT, Chang CM. Applications of dual MRM for determining the natural frequencies and natural modes of an Euler–Bernoulli beam using the singular value decomposition method. Eng Anal Bound Elem 1999;23:339–60.
[11] Yeih W, Chang JR, Chang CM, Chen JT. Applications of dual MRM for determining the natural frequencies and natural modes of a rod using the singular value decomposition method. Adv Eng Software 1999;30:459–68.
[12] Chen JT, Kuo SR, Chung IL, Huang CX. Study on the true and spurious eigensolutions of two-dimensional cavities using the multiple reciprocity method. Eng Anal Bound Elem 2003;27:655–70.
[13] Chen JT, Liu LW, Hong HK. Spurious and true eigensolutions of Helmholtz BIEs and BEMs for a multiply-connected problem. Proc R Soc London Ser A 2003;459:1891–925.
[14] Chen JT, Chen IL, Chen KH. Treatment of rank deficiency in acoustics using SVD. J Comput Acoust 2006;14:157–83.
[15] Schroeder W. The origin of spurious modes in numerical solutions of electromagnetic field eigenvalue problems. IEEE Trans Microwave Theory Tech 1994;42:644–53.
[16] Hartmann F. Introduction to boundary elements—theory and applications. Berlin: Springer; 1989.
[17] Banerjee PK, Butterfield R. Boundary element methods in engineering science. London: McGraw-Hill; 1981.
[18] Chen JT, Chou KS, Hsieh CC. Derivation of stiffness and flexibility for rods and beams by using dual integral equations. Eng Anal Bound Elem 2008;32:108–21.
[19] Providakis CP, Beskos DE. Dynamic analysis of beams by the boundary element method. Comput Struct 1986;22(6):957–64.
[20] Sapountzakis EJ, Tsiatas GC. Flexural–torsional vibrations of beams by BEM. Comput Mech 2007;39:409–17.
[21] Tai GRC, Shaw RP. Helmholtz-equation eigenvalues and eigenmodes for arbitrary domains. J Acoust Soc Am 1974;56(3).
[22] De Mey G. Calculation of eigenvalues of the Helmholtz equation by an integral equation. Int J Numer Method Eng 1976;10:59–66.
[23] De Mey G. A simplified integral equation method for the calculation of the eigenvalues of Helmholtz equation. Int J Numer Method Eng 1977;11:1340–2.

[24] Hutchinson JR. Boundary method for time-dependent problems. In: Proceedings of the fifth engineering mechanics division conference, ASCE, WY; 1984. p. 136–9.
[25] Hutchinson JR, Wong GKK. The boundary element method for plate vibrations. In: Proceedings of the ASCE seventh international conference on electronic computation; 1979. p. 297–311.
[26] Yasko M. BEM with the real-valued fundamental solutions for the Helmholtz equation. In: Proceedings of the seventh international congress of sound and vibration, Germany; 2000. p. 2037–44.
[27] Duran M, Miguez M, Nedelec JC. Numerical stability in the calculation of eigenfrequencies using integral equations. J Comput Appl Math 2001;130:323–36.
[28] Kang SW, Lee JM, Kang YJ. Vibration analysis of arbitrarily shaped membranes using non-dimensional dynamic influence function. J Sound Vib 1999;234(1):455–70.
[29] Chen JT, Chang MH, Chung IL, Cheng YC. Comment on "Eigenmode analysis of arbitrarily shaped two-dimensional cavities by the method of point matching". J Acoust Soc Am 2002;111(1 Part 1).
[30] Chen JT, Lee CF, Lin SY. A new point of view for the polar decomposition using singular value decomposition. Int J Comp Numer Anal Appl 2002;2(3):257–64.
[31] Chen IL, Chen JT, Liang MT. Analytical study and numerical experiments for radiation and scattering problems using the CHIEF method. J Sound Vib 2001;248(5):809–28.
[32] Chen JT, Chen IL, Kuo SR, Liang MT. A new method for true and spurious eigensolutions of arbitrary cavities using the combined Helmholtz exterior integral equation formulation method. J Acoust Soc Am 2001;109(3):982–98.
[33] Chen JT, Hong HK. Boundary element method. Taipei: New World Press; 1992 [in Chinese].
[34] Hong HK, Chen JT. Derivation of integral equations in elasticity. J Eng Mech ASCE 1988;114:1028–44.
[35] Chen JT, Hong HK. Review of dual boundary element methods with emphasis on hypersingular integrals and divergent series. Appl Mech Rev ASME 1999;52(1):17–33.
[36] Chen JT, Chen WC, Lin SR, Chen IL. Rigid body mode and spurious mode in the dual boundary element formulation for the Laplace problems. Comput Struct 2003;81:1395–404.
[37] Lee WM, Chen JT. Analytical study and numerical experiments of true and spurious eigensolutions of free vibration of circular plates using real-part of BIEM. Eng Anal Bound Elem 2008;32:368–87.

Please cite this article as: Chen JT, et al. On the spurious eigensolutions for the real-part boundary element method. Eng Anal Bound Elem (2008), doi:10.1016/j.enganabound.2008.07.003